Translational Oncology 32 (2023) 101649

Contents lists available at ScienceDirect

Translational Oncology

journal homepage: www.elsevier.com/locate/tranon

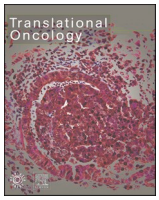

Original Research

Downregulation of miR-221–3p promotes the ferroptosis in gastric cancer cells via upregulation of ATF3 to mediate the transcription inhibition of GPX4 and HRD1

Chang-Jiang Shao [a,b], Hai-Lang Zhou [c], Xu-Zhu Gao [d], Chun-Fang Xu [a,*]

[a] Department of Gastroenterology, The First Affiliated Hospital of Soochow University, Suzhou 215006, Jiangsu Province, PR China
[b] Department of Gastroenterology, Lianyungang Cancer Hospital, The Second People's Hospital of Lianyungang City, Lianyungang 222006, Jiangsu Province, PR China
[c] Department of Gastroenterology, The people's Hospital of Lianshui County, Huaian 223400, Jiangsu Province, PR China
[d] Central laboratory, Lianyungang Cancer Hospital, The Second People's Hospital of Lianyungang City, Lianyungang 222006, Jiangsu Province, PR China

ARTICLE INFO

Keywords:
Gastric cancer
miR-221–3p
ATF3
Ferroptosis
HRD1
GPX4

ABSTRACT

Background: Gastric cancer (GC) is an aggressive gastrointestinal tumor. MiRNAs participate in the tumorigenesis of GC. Nevertheless, the function of miR-221–3p in GC remains largely unknown.
Methods: RNA levels were assessed by RT-qPCR. Western blot was performed to test the protein levels. The relation between miR-221–3p and ATF3 was investigated by dual-luciferase reporter assay. ChIP and dual-luciferase reporter assay were applied to assess the interaction between ATF3 and HRD1 or GPX4. Meanwhile, cell proliferation was investigated by CCK8 and colony formation assay. The content of erastin-induced Fe^{2+} was investigated by iron assay kit. Erastin-induced lipid ROS level was assessed by C11-BODIPY 581/591. Co-immunoprecipitation was used to detect the interaction between HRD1 and ACSL4. In addition, xenograft mice model was established to detect the effect of miR-221–3p in GC.
Results: Depletion of miR-221–3p greatly attenuated GC cell proliferation through promoting ferroptosis. Meanwhile, ATF3 was downregulated in GC, and it was identified to be the downstream mRNA of miR-221–3p. MiR-221–3p downregulation could promoted the ferroptosis in GC cells through upregulation of ATF3. HRD1 mediates ubiquitination and degradation of ACSL4 to inhibit ferroptosis. ATF3 upregulation could reduce GC cell proliferation via downregulating the transcription of GPX4 and HRD1. Furthermore, downregulation of miR-221–3p markedly attenuated the growth of GC in mice.
Conclusion: HRD1 mediates ubiquitination and degradation of ACSL4 to inhibit ferroptosis. MiR-221–3p depletion upregulates the ferroptosis in GC cells via upregulation of ATF3 to mediate the transcription inhibition of GPX4 and HRD1. Our study might provide a novel target for GC treatment.

Introduction

Gastric cancer (GC) is a prevalent cancer in the digestive system [1]. Its incidence stood up to 8% of malignant tumor [2]. The prognosis is largely poor because of the distant metastasis, and it stands up to over 80% of tumor-caused deaths [3]. Surgical resection is the main treatment against primary tumor, while the therapeutic effect is still not ideal [4]. Hence, it is essential to discover the pathogenesis of GC. Ferroptosis is an iron-dependent mechanism of cell death [5]. It is a programmed cell death process which is not the same as necrosis, autophagy, and apoptosis [6,7]. Accumulating evidence indicate that ferroptosis is a key tumor suppression mechanism by silencing genes involved in the initiation and execution of necroptosis in cancers [8]. Guan Z et al. showed that Tanshinone IIA could inhibit the tumorigenesis of GC via promoting the ferroptosis [9]; Hao S et al. indicated that cysteine dioxygenase 1 could modulate erastin-induced ferroptosis in GC [10]. Thus, ferroptosis could play a vital role in GC treatment.

MicroRNAs (miRNAs) are confirmed to modulate the mRNA

Abbreviation: GC, gastric cancer; ACSL4, acyl-coenzyme A synthetase long chain member 4; ATF3, activating transcription factor 3; GPX4, glutathione peroxidase 4; ROS, reactive oxygen species; miRNA, microRNA; HRD1, 3-Hydroxy-3-methylglutaryl reductase degradation.

* Corresponding author at: Department of Gastroenterology, The First Affiliated Hospital of Soochow University, No.188, Shizi Street, Suzhou 215006, Jiangsu Province, PR China.
E-mail address: xcf304@163.com (C.-F. Xu).

https://doi.org/10.1016/j.tranon.2023.101649
Received 16 November 2022; Received in revised form 14 December 2022; Accepted 24 February 2023
Available online 21 March 2023

expression by regulation mRNA decay [11]. Additionally, it was revealed that miRNAs can act as key modulators in various diseases, such as inflammatory diseases and cancers [12,13]. Meanwhile, previous studies showed that miRNAs participate in the progression of GC. CH et al. revealed that miR-27b-3p could suppress the migration, invasion and EMT process in GC through targeting RUNX1 [14]. miR-221–3p was known to be an oncogene as it could promote the tumorigenesis of GC. For example, miR-221–3p played a critical role in GC by suppressing PTEN or LIFR expression [15,16]. It has been reported that serum miR-221–3p was involved in the development of GC and had important clinical values in gastric cancer diagnosis and prognosis [17]. Whether miR-221–3p regulates ferroptosis in GC progression is still unknown.

Activating transcription factor 3 (ATF3), as a member of the ATF/cyclic AMP response element-binding (ATF/CREB) family of transcription factors, is a stress-induced transcription factor that plays crucial roles in regulating metabolism, immune response, and oncogenesis [18]. It has been reported that GC patients with low expression of ATF3 had poorer survival and prognosis [19]. In this study, ATF3 might be the downstream of miR-221–3p in the prediction of starbase dataset. Nevertheless, the correlation between miR-221–3p and ATF3 in GC cells needs to be further investigated.

Glutathione peroxidase 4 (GPX4) is involved in the activation of ferroptosis as it plays a key role in iron-catalyzed lipid oxidative injury [20,21]. In addition, it has been reported that GPX4 is an inhibitor of ferroptosis [22,23]. Moreover, a previous report suggested ATF3 could negatively regulate GPX4 [24]. However, the function and the interaction between ATF3 and GPX4 in GC remains unknown.

3-Hydroxy-3-methylglutaryl reductase degradation (HRD1, also known as SYVN1), an E3 ubiquitin ligase, is involved in endoplasmic reticulum (ER)-associated degradation (ERAD) [25]. It was reported that HRD1 was upregulated in a variety of tumor tissues, such as lung cancer, hepatocellular carcinoma and GC [26,27]. Accumulated evidence demonstrated that HRD1 mediated various proteins ubiquitination for promoting cancer progression. For example, HRD1 targeted PTEN for ubiquitination and degradation to promote hepatocellular carcinoma progression [26]. HRD1 promoted lung cancer by interacting with SIRT2 and mediating its ubiquitination and degradation [27]. However, the role of HRD1 in GC remains mysterious.

Acyl-coenzyme A synthetase long chain member 4 (ACSL4) is a key regulator in fatty acid catabolism. ACSL4 is known to be the important mediator in ferroptosis as ACSL4 upregulation could induce the ferroptosis [23,28]. A previous report indicated that ACSL4 was downregulated in GC [29]. UbiBrowser database predicts that ACSL4 is a substrate of E3 ligase HRD1. However, the detailed function of ACSL4 in GC remains to be further explored.

In this study, we found that HRD1 mediated ubiquitination and degradation of ACSL4 to inhibit ferroptosis and miR-221–3p knockdown promoted the ferroptosis in GC cells via targeting ATF3 to mediate the transcription inhibition of GPX4 and HRD1. Our study might supply novel insights on discovering the methods against GC.

Material and methods

Patients sample

Thirty-two pairs of GC adjacent normal tissues were provided by The First Affiliated Hospital of Soochow University from April 2019 to July 2020. All cases were independently diagnosed histologically by two experienced pathologists. No patient was given radiotherapy or chemotherapy before surgery. All tissue samples were immediately frozen in liquid nitrogen after resection from GC patients and then were stored at −80°C. All the patients ($n = 32$) signed the informed consent before the experiments. The Ethics Committee of The First Affiliated Hospital of Soochow University approved this research.

Cell culture

GC cells (MKN45, AGS, MGC803 and MKN-7), GES-1 and 293T cells were purchased from ATCC and maintained in DMEM containing FBS (10%), streptomycin and penicillin (1%, Thermo Fisher Scientific) at 37°C and 5% CO_2. For assessing the function of ferroptosis in GC, GC cells were exposed to 10 μg/mL erastin (Selleck Chemicals, #S7242) [10], or ferroptosis inhibitor ferrostain-1 (Fer-1, 2 mM; Abcam) [30] for 48 h.

Cell transfection

MiR-221–3p mimics/inhibitor, sh-ATF3, sh-HRD1, pcDNA3.1-ATF3 (oe-ATF3), and corresponding negative vector (mimic/inhibitor NC, sh-NC, oe-NC) originated from GenePharma. The cells in the exponential phase of growth were seeded in 6-well plates at a density of 1×10^5 cells per well and grown for 24 h. And then the cells were transfected with above plasmid by Lipofectamine 3000 (Invitrogen) and maintained in OPTI-MEM. Finally, the cells were harvested for detection after 48 h post transfection.

RT-qPCR assay

TRIzol reagent was applied to isolate RNA from tissues or cells. PrimeScript RT reagent Kit (Takara) was applied to synthesize cDNA. SYBR Green methods was applied in RT-qPCR using ABI7500 system. $2^{-\triangle\triangle CT}$ method was applied in quantification. β-actin and U6 were applied as internal control. The primers originated from GenePharma. ATF3: forward, 5-CTCCTGGGTCACTGGTGTTT-3′ and reverse 5′-GCTACCTCGGCTTTTGTGAT-3′. miR-221–3p: forward, 5′- CGGCTACATTGTCTGCCTG-3′ and reverse 5′-CAGTGCGTGTCGTGGAGT-3′. β-actin: forward, 5′-CCCTGGAGAAGAGCTACGAG-3′ and reverse 5‘-CGTACAGGTCTTTGCGGATG-3′. GPX4: forward, 5‘-GTAACCAGTTCGGGAAGCAG-3′ and reverse 5‘-TGTCGATGAGGAACTGTGGA-3′. HRD1: forward, 5‘- CCAACATCTCCTGGCTCTTTCAC-3′ and reverse 5‘- GTCAGGATGCTGTGATAGGCGT-3′. U6: forward, 5′-CTCGCTTCGGCAGCACA-3′ and reverse 5′-AACGCTTCACGAATTTGCGT-3′.

Western blotting

RIPA (Beyotime) was applied to isolate total protein from cells. BCA protein kit (Thermo Fisher Scientific) was applied to assess the protein concentration. SDS-PAGE gel (10%) was applied to separate the proteins and then proteins were transferred onto PVDF (Beyotime) membranes. The primary antibodies were applied to incubate the membranes overnight after blocking for 1 h. Then, the corresponding secondary antibody (1:5000, ab7090, Abcam) was applied to incubate the membranes for 1 h. ECL kit (Invitrogen) was applied to visualize the protein bands. The primary antibodies were purchased from Abcam as follows: anti-GPX4 (1:1000, ab125066), anti-HRD1 (1:1000, ab170901), anti-ACSL4 (1:1000, ab155282), anti-ATF3 (1:1000, ab207434) and anti-GAPDH (1:10000, ab181602). GAPDH was regarded as an internal control.

Dual luciferase reporter assay

To investigate the relationship between miR-221–3p and ATF3, wild-type or mutant type ATF3 3′UTR (WT/MUT) including the binding sites of miR-221–3p, originated from Beyotime, then were cloned into the psiCHECK2 (Promega, Madison, WI, USA). The ATF3 3′UTR (WT/MUT) psiCHECK2 were added into 293T cells with miR-221–3p/NC mimics by using Lipofectamine 3000. Cells were harvested after 48 h post transfection and detected by the Dual-Glo Luciferase Assay System (Promega).

To verify the transcriptional regulation of GPX4 and HRD1 by ATF3, GPX4 or HRD1 promoter were cloned into the psiCHECK2. The 293T

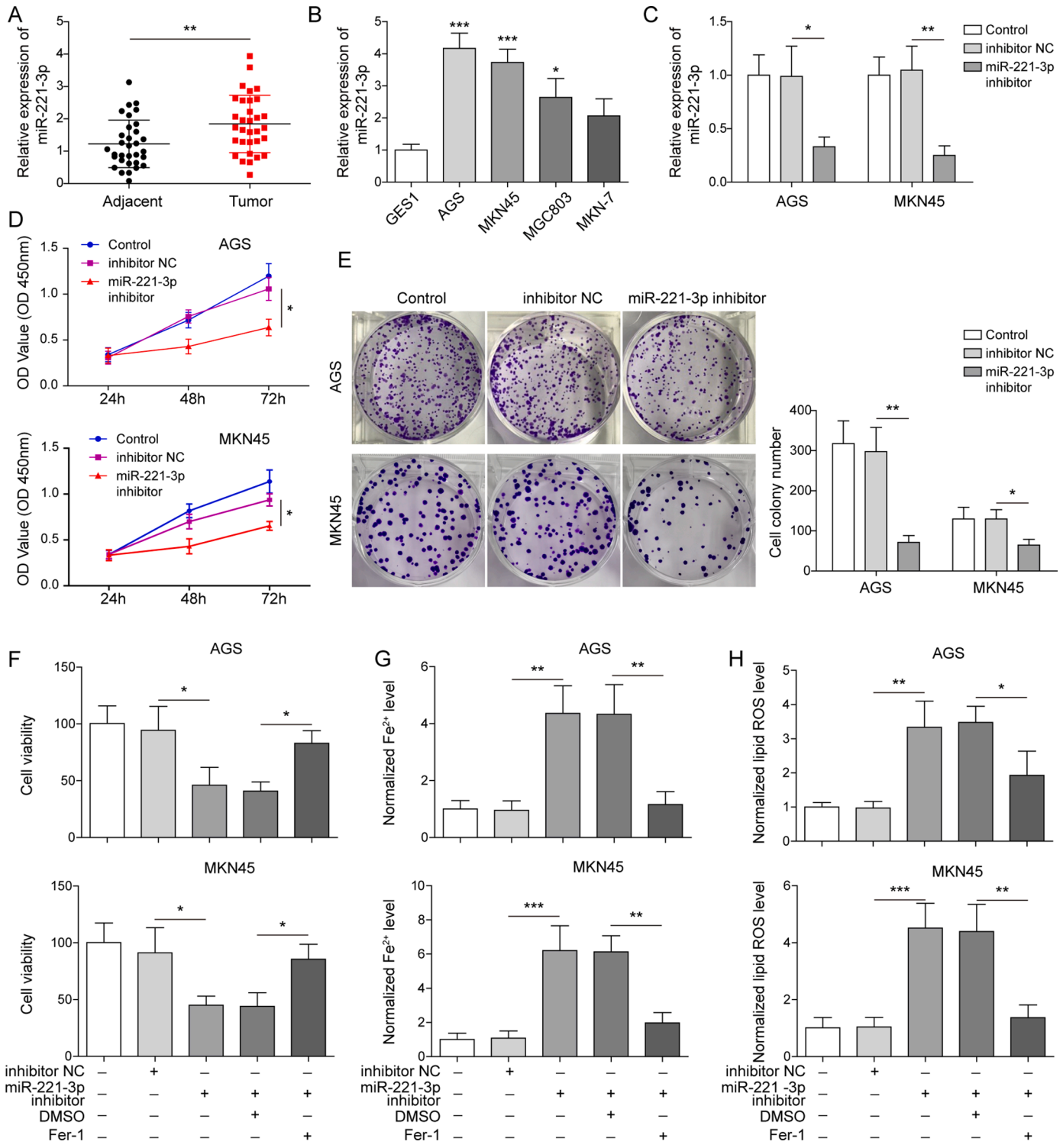

Fig. 1. MiR-221–3p downregulation attenuates GC cell proliferation via inducing the ferroptosis. (A) MiR-221–3p level in GC or normal tissues was investigated by RT-qPCR. (B) MiR-221–3p level was investigated by RT-qPCR. (C) AGS or MKN45 cells were treated with inhibitor NC or miR-221–3p inhibitor. MiR-221–3p level in GC cells was investigated by RT-qPCR. (D) GC cell viability was assessed by CCK8 assay. (E) Colony formation assay was applied to assess the cell proliferation. (F) CCK8 assay was applied to assess the viability. (G) The content of Fe^{2+} in GC cells was investigated by iron analysis kit. (H) The ROS level in GC cells was evaluated by flow cytometry. *$p<0.05$, **$p<0.01$, ***$p<0.001$.

cells were co-transfected with GPX4 or HRD1 promoter vectors and oe-NC or oe-ATF3 by Lipofectamine 3000. The relative luciferase activities were tested by the Dual-Glo Luciferase Assay System (Promega).

ChIP assay

To detect the binding between ATF3 and HRD1/GPX4 promoter, ChIP Assay Kit (Millipore) was applied in ChIP detection. Briefly, the cells were treated with a lysis buffer on ice for 10 min. Subsequently, the cell lysates were then sonicated for seven five-second pulses on ice using

Table 1
miR-221–3p expression and clinical features of patients with gastric cancer.

Clinical features	miR-221–3p High	Low	P value
No.	15	17	
Gender			
Male	8	8	0.7232
Female	7	9	
Age			
<60 years	9	8	0.4641
≥60 years	6	9	
Tumor size			
<5cm	5	12	0.0351*
≥5cm	10	5	
Tumor differentiation			
Well+moderate	6	13	0.0361*
Poor+undifferentiated	9	4	
T stage			
T_1+T_2	7	10	0.4916
T_3+T_4	8	7	
N stage			
N_0+N_1	6	12	0.0818
N_2+N_3	9	5	
M stage			
M0	4	10	0.0141*
M1	13	5	
TNM stage			
I+II	4	14	0.0015*
III+IV	11	3	

* $p<0.05$.

a microsonicator tip (Qsonica). This sonication procedure resulted in 200–1000 bp DNA fragments. Subsequently, cell lysates were treated with ChIP buffer, ProteinA Agarose and protease inhibitor cocktail on ice for 30 min. Mixture was then incubated with antibodies against ATF3 (ab207434, Abcam), or mouse IgG (ab37355, Abcam) at 4 °C for 12 h. Next, the mixture was washed with eluate buffer. The cross-linking was reversed by 5 M NaCl followed by incubation at 65 °C overnight. Finally, the samples were treated with RNaseA and then used for PCR.

Co-immunoprecipitation (IP) assay

Co-IP experiment was performed as described [31]. The cells were lysed in lysis buffer (0.5% Triton-X-100, 150 mM NaCl, 12.5 mM β-glycerolphosphate, 1.5 mM $MgCl_2$, 2 mM EGTA, 10 mM NaF, 1 mM Na_3VO_4, 2 mM DTT) containing protease inhibitors. The lysates were centrifuged at 12,000 × g for 10 min at 4 °C. For each immunoprecipitation, the supernatant was incubated with 35 μL of 50% slurry of Protein A/G Sepharose (Amersham) and 0.5 μg anti-ACSL4 for at least 12 h. After washing the beads with PBS three times, immunoprecipitates were analyzed by Western blot analysis.

Cell viability assay

The viability of GC cells was assessed in each group using the CCK-8 assay (Beyotime Institute of Biotechnology) as described [32]. In brief, GC cells were plated (5×10^3 cells/well) into 96-well plates and treated for 0, 24, 48 or 72 h. Afterwards, CCK-8 (10 μL) was added to the cells for 2 h at 37 °C. The absorbance (450 nm) was assessed by a microplate reader (Tecan).

Colony formation assay

The treated cells were seeded (500 cells/well) into 6-well plate and cultured in a 37 °C incubator for two weeks. Subsequently, the colonies were fixed by 4% PFA for 10 min. After that, crystal violet (1%) was applied to stain the colonies for 5 min. Finally, the result was calculated by a light microscope (Leica).

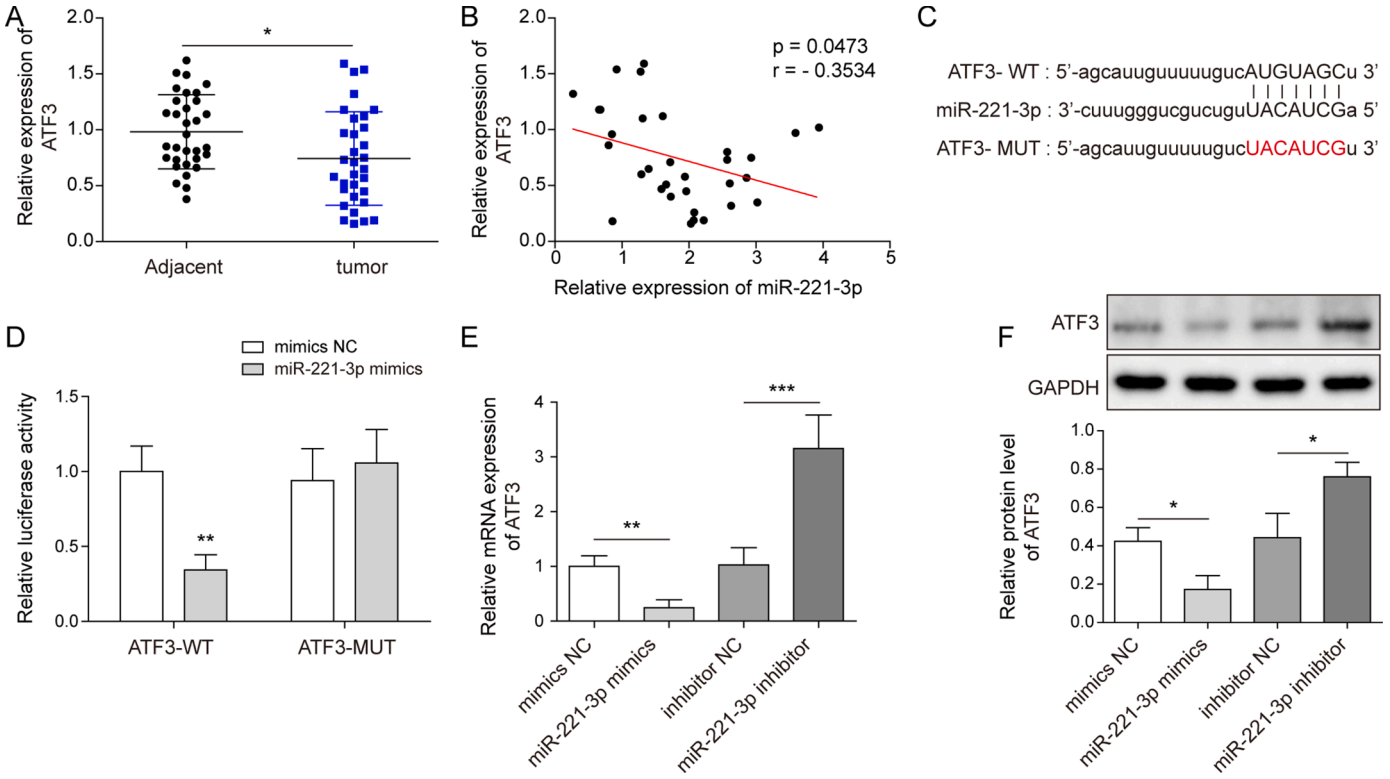

Fig. 2. MiR-221–3p directly targets ATF3 in GC cells. (A) ATF3 level in GC or normal tissues was investigated by RT-qPCR. (B) The correlation among miR-221–3p and ATF3 in GC was analyzed. (C) The downstream of miR-221–3p was predicted by TargetScan. (D) Dual luciferase assay was applied to assess the targeted relationship between miR-221–3p and ATF3. (E) ATF3 level in GC cells was tested by RT-qPCR. (F) ATF3 level in GC cells was examined by western blot. GAPDH was applied for normalization. *$p<0.05$, **$p<0.01$, ***$p<0.001$.

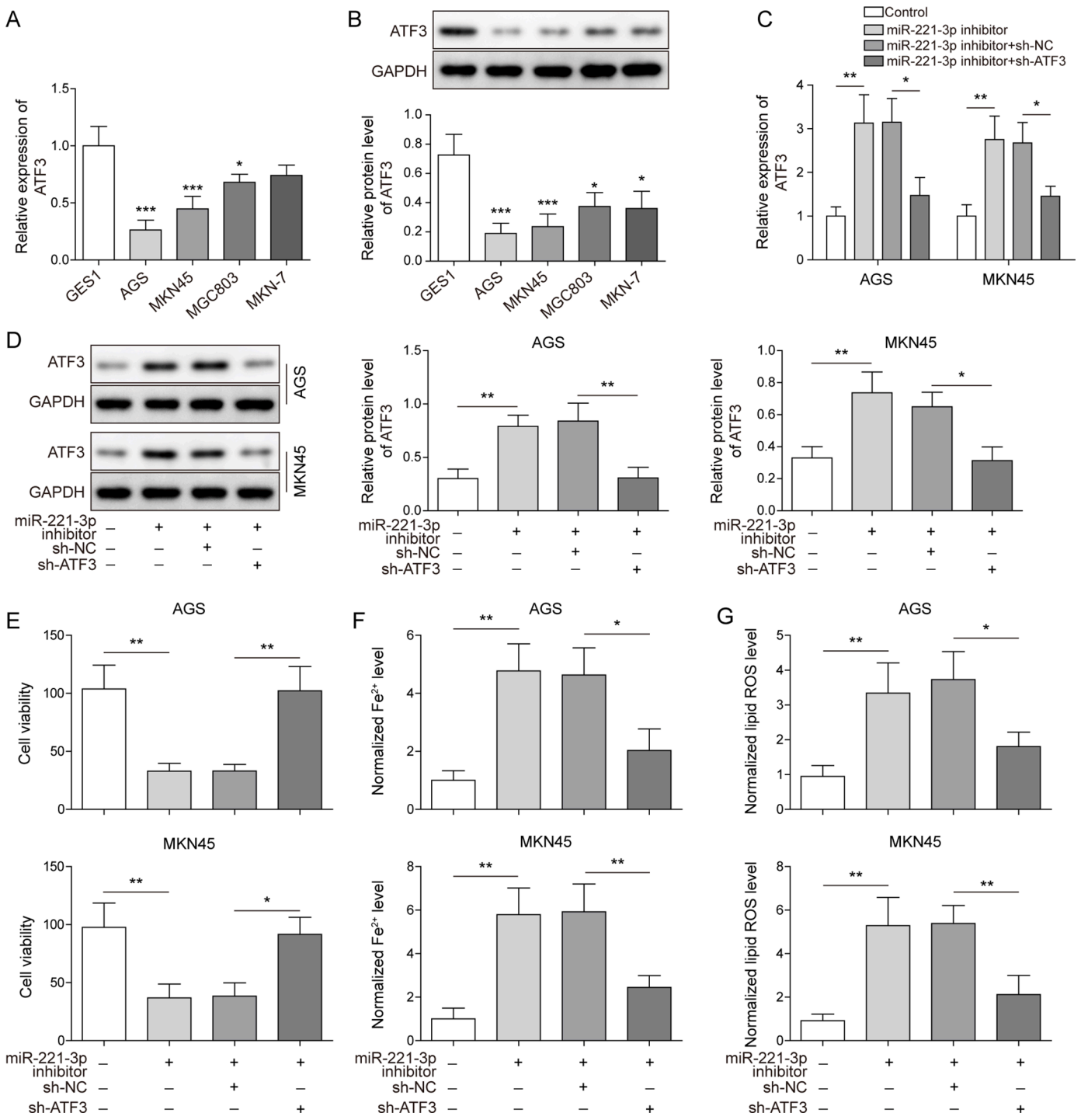

Fig. 3. MiR-221–3p regulates the proliferation of GC cells through targeting ATF3. (A, B) ATF3 level was investigated by RT-qPCR and western blot. (C, D) ATF3 level in GC cells was assessed by RT-qPCR and western blot. GAPDH was applied for normalization. (E) GC cell viability was assessed by CCK8 assay. (F) The content of Fe^{2+} in GC cells was assessed by iron analysis kit. (G) Flow cytometry was applied to assess the ROS level. *$p<0.05$, **$p<0.01$, ***$p<0.001$.

Iron assay

Iron assay kit (Abcam) was used to detect iron concentration as described [33]. According to the manufacturer's instructions, the GC cells were collected and homogenized in 5 × volume of iron assay buffer on ice, and then the cells were centrifuged at 13,000 × g for 10 min at 4 °C, to obtain the supernatant. After that, the iron assay buffer (50 μL) was applied to incubate the supernatant in a microplate (96-well) for 30 min. Then, reagent mix was applied to incubate the buffer (50 μL) for 30 min without light. The microplate reader (Tecan) was applied to assess the absorbance at 593 nm.

Lipid reactive oxygen species (ROS) detection

C11-BODIPY 581/591 (Thermo Fisher) was applied to assess the lipid ROS level as described [34]. Briefly, cells were trypsinized and then resuspended in 400 μL of serum-free medium with BODIPYTM 581/591 C11 (2 μM). And then cells were incubated at 37 °C for 30 min in a cell culture incubator. Fluorescence emission peaks were analyzed by a flow cytometer (BD). The peak from 510 to 590 nm is proportional to lipid

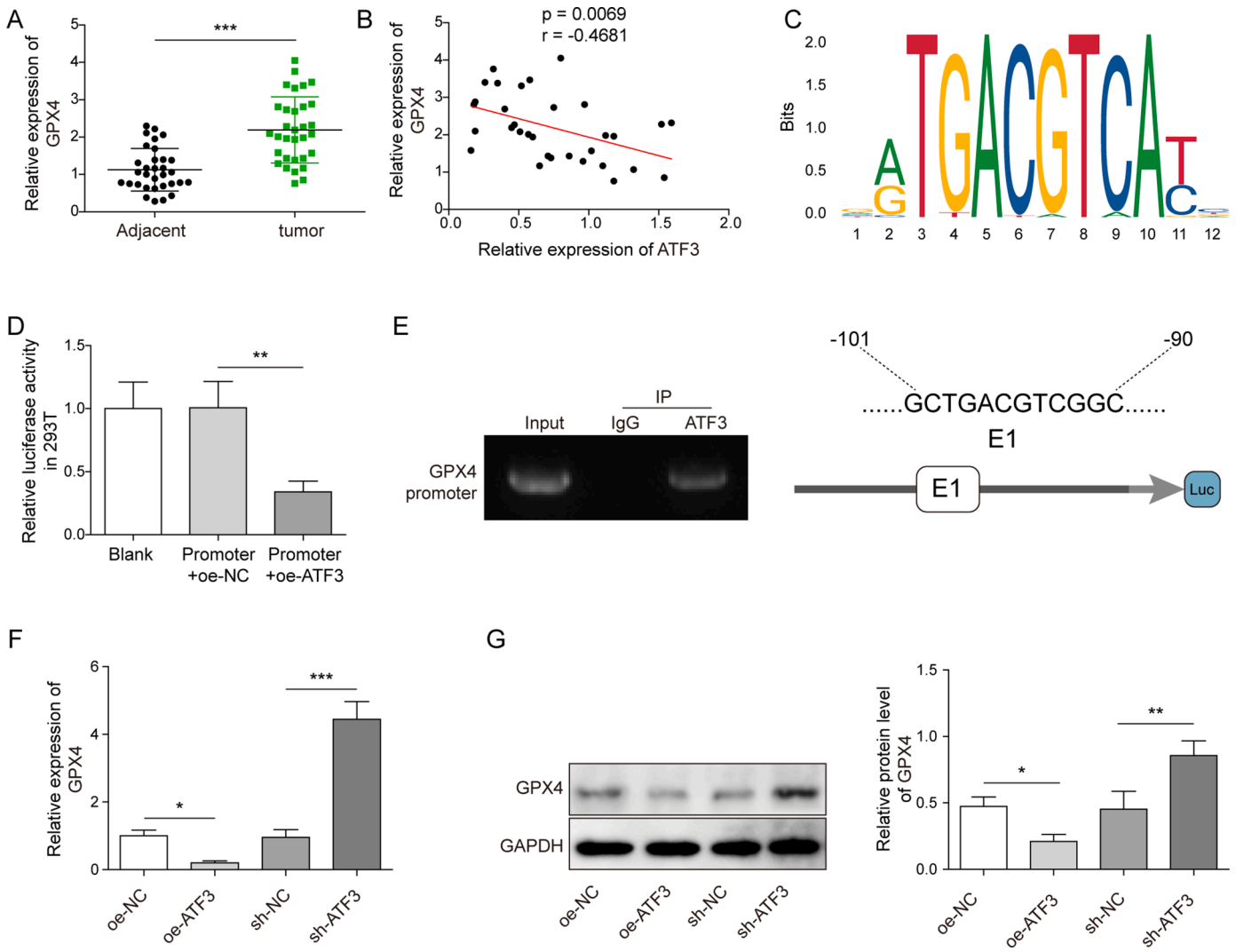

Fig. 4. ATF3 inhibits the transcription of GPX4. (A) The level of GPX4 in GC and normal tissues was investigated by RT-qPCR. (B) The correlation among GPX4 and ATF3 in GC was analyzed. (C) The potential binding sites between ATF3 and GPX4 were predicted by JASPAR. (D) The luciferase activity was tested by dual luciferase report assay. (E) GPX4 promoter enrichment was tested by ChIP. (F, G) GPX4 level in GC cells was tested by RT-qPCR and western blot. *p<0.05, **p<0.01, ***p<0.001.

ROS generation.

Animal model

Animal experiments were performed as described [35]. BALB/c nude mice (n = 5, 6–8 weeks old) originated from Vital River (Beijing, China). Mice were placed in condition of dedicated SPF. MiR-221–3p downregulated MKN45 cells (5 × 10^6 cells per mouse), which were infected with lentivirus containing anti-miR-221–3p, were transplanted subcutaneously in each mouse. The tumor volume was assessed every week. After 4 weeks, mice were sacrificed for tumor collection. All *in vivo* experiments were performed in line with NIH guide, and Ethics Committees of The First Affiliated Hospital of Soochow University approved this study.

Statistical analysis

Data are presented as the mean ± SD. At least three independent experiments were applied in each group. Student's t-test was applied to compare the difference between 2 groups. One-way ANOVA followed by Tukey's post hoc test (GraphPad Prism; version 7) was applied to analyze the difference among multiple groups. $p < 0.05$ was considered as statistically significant.

Results

Downregulation of miR-221–3p inhibits GC cell proliferation via promoting the ferroptosis

In Fig. 1A, miR-221–3p level in GC tissues was greatly higher than that in normal tissues. Additionally, miR-221–3p level was notably upregulated in tumor cells than that in GES-1 cells (Fig. 1B). Since AGS and MKN45 cells were more sensitive to miR-221–3p level, these two cells were selected in subsequent analysis. MiR-221–3p level in GC cells was greatly downregulated by miR-221–3p inhibitor (Fig. 1C). MiR-221–3p downregulation significantly attenuated GC cell proliferation and viability (Fig. 1D and 1E). Meanwhile, miR-221–3p inhibitor-induced cell viability reduction was notably restored by Fer-1 (Fig. 1F). Consistently, the content of erastin-induced Fe^{2+} in GC cells was markedly promoted by miR-221–3p inhibitor, which was reversed by Fer-1 (Fig. 1G). Furthermore, miR-221–3p inhibitor-caused upregulation of erastin-induced ROS was partially abolished by Fer-1 (Fig. 1H). Besides, miR-221–3p level was related with the size of tumor, differentiation and TNM stage in GC patients (Table 1). Taken together, miR-

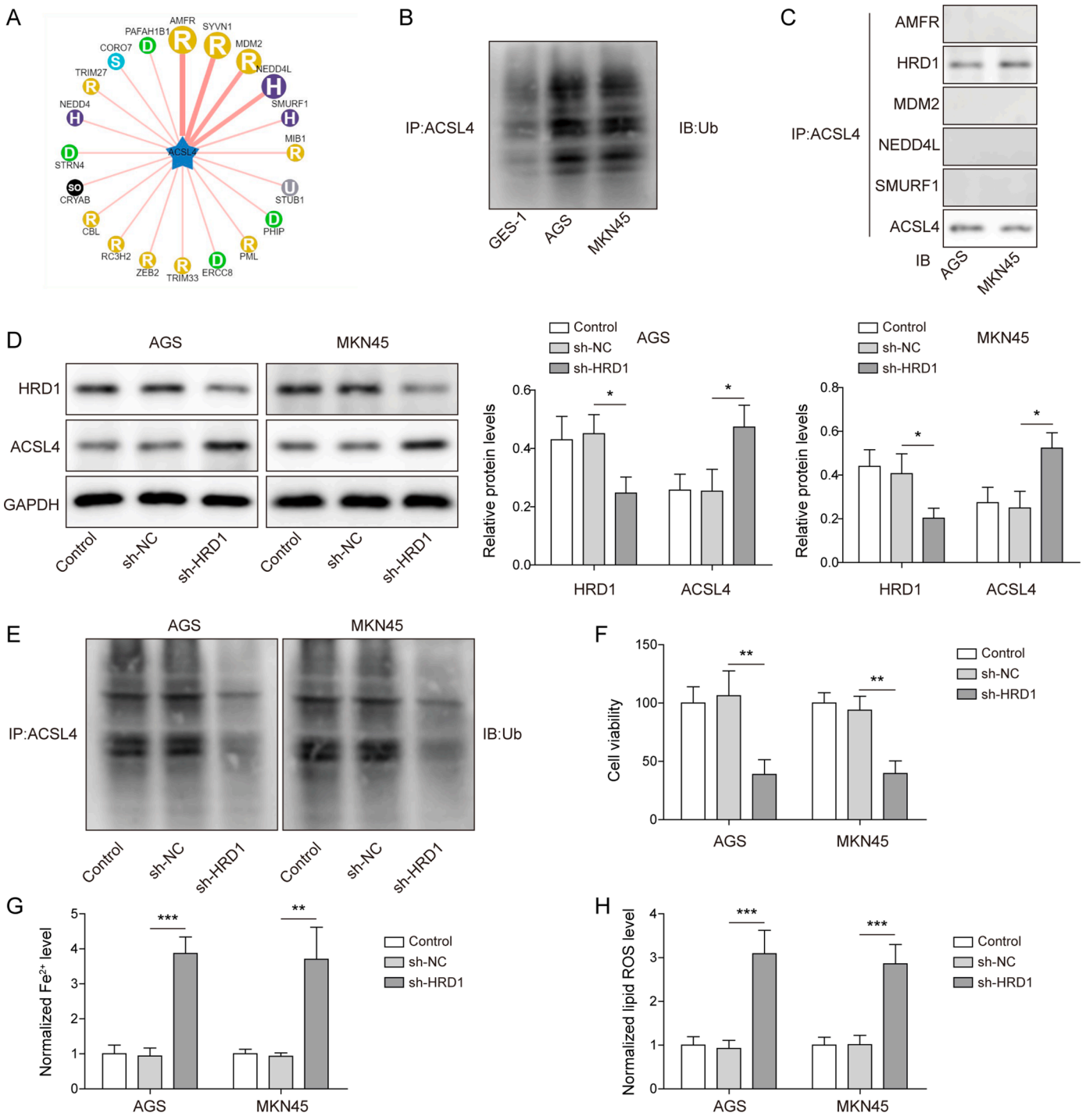

Fig. 5. HRD1 mediates ubiquitination and degradation of ACSL4. (A) ACSL4 is a substrate of E3 ligases by UbiBrowser database. (B) The ubiquitination level of ACSL4 in GC cells and GES-1 cells. (C) HRD1 interacted with ACSL4 by immunoprecipitation experiment. (D) Effect of knockdown of HRD1 on expression level of ACSL4. (E) Effect of knockdown of HRD1 on ubiquitination level of ACSL4. (F) GC cell viability was assessed by CCK8 assay. (G) The content of Fe2+ in GC cells was assessed by iron analysis kit. (H) The ROS level in GC cells was evaluated by flow cytometry. *$p<0.05$, **$p<0.01$, ***$p<0.001$.

221–3p downregulation inhibited GC cell proliferation via facilitating the ferroptosis.

MiR-221–3p directly targets ATF3

As indicated in Fig. 2A, the level of ATF3 in GC tissues were much lower than that in normal tissues. Additionally, miR-221–3p level in GC tissues was negatively associated with ATF3 (Fig. 2B). MiR-221–3p had binding sites with ATF3 mRNA (Fig. 2C), and the relative luciferase activity of ATF3-WT was notably decreased by miR-221–3p overexpression (Fig. 2D). Furthermore, ATF3 level in GC cells was negatively modulated by miR-221–3p (Fig. 2E and 2F). Taken together, miR-221–3p directly targeted ATF3 in GC cells.

MiR-221–3p regulates the ferroptosis of GC cells by targeting ATF3

The results demonstrated that ATF3 level in GC cells was much lower, compared with that in GES-1 cells (Fig. 3A and 3B). Meanwhile,

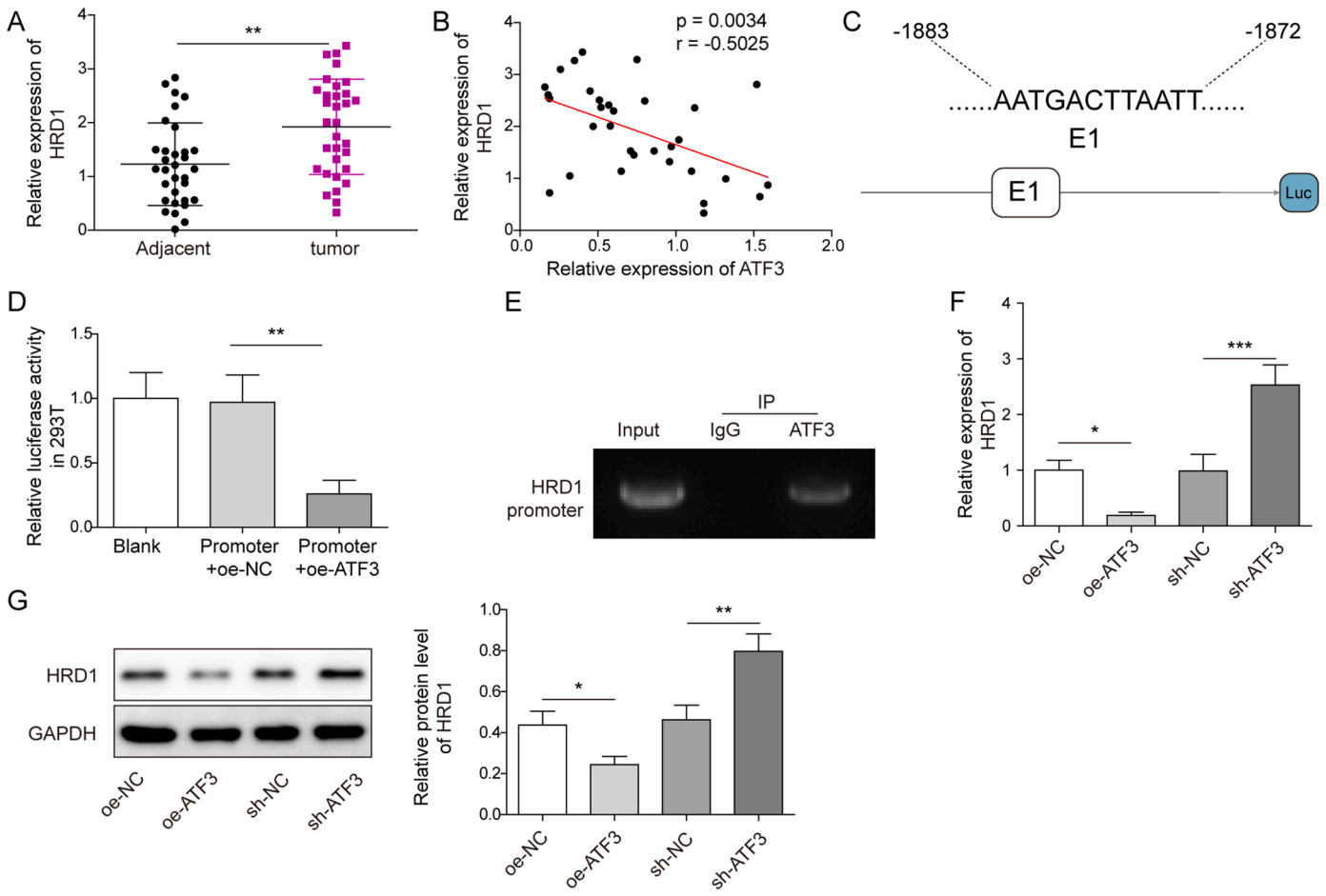

Fig. 6. ATF3 inhibits the transcription of HRD1. (A) The level of HRD1 in GC and normal tissues was investigated by RT-qPCR. (B) The correlation among HRD1 and ATF3 in GC was analyzed. (C) The potential binding sites between ATF3 and HRD1 were predicted by JASPAR. (D) Dual luciferase assay was applied to assess the targeted relationship between HRD1 and ATF3. (E) HRD1 promoter enrichment was tested by ChIP. (F, G) HRD1 level in GC cells was tested by RT-qPCR and western blot. *$p<0.05$, **$p<0.01$, ***$p<0.001$.

miR-221–3p inhibitor-induced upregulation of ATF3 was reversed by ATF3 knockdown (Fig. 3C and 3D). Additionally, ATF3 silencing reversed miR-221–3p inhibitor-induced suppression of cell viability (Fig. 3E). Furthermore, the content of erastin-induced Fe^{2+} in miR-221–3p inhibitor-treated GC cells was markedly decreased by ATF3 knockdown (Fig. 3F). Consistently, the erastin-induced ROS level in miR-221–3p inhibitor-treated cells was significantly downregulated by ATF3 knockdown (Fig. 3G). Collectively, miR-221–3p regulated the ferroptosis of GC cells through targeting ATF3.

ATF3 inhibits the transcription of GPX4

As indicated in Fig. 4A, the level of GPX4 in GC tissues was much higher, compared with that in normal tissues, and GPX4 level in GC tissues was negatively with ATF3 (Fig. 4B). On the other hand, GPX4 had potential binding site (E1) with ATF3, and overexpression of ATF3 significantly decreased the luciferase activity in GPX4 promoter region (Fig. 4C and 4D). In addition, the enrichment of GPX4 promoter was significantly increased by ani-ATF3 (Fig. 4E). Meanwhile, GPX4 level in GC cells was negatively regulated by ATF3 (Fig. 4F and 4G). Taken together, ATF3 inhibited the transcription of GPX4.

HRD1 mediates ubiquitination and degradation of ACSL4

The UbiBrowser database predicts that ACSL4 is a substrate of E3 ligases (Fig. 5A). Next, we detected ubiquitination level of ACSL4 in GC cells and GES-1 cells. The result showed that ubiquitination level of ACSL4 in gastric cancer cells was obviously increased compared to GES-1 (Fig. 5B). Immunoprecipitation experiments showed that HRD1 interacted with ACSL4 (Fig. 5C). Knockdown of HRD1 enhanced the level of ACSL4 (Fig. 5D). Knockdown of HRD1 inhibited ubiquitination level of ACSL4 (Fig. 5E). In addition, knockdown of HRD1 suppressed GC cell viability (Fig. 5F). The level of erastin-induced Fe^{2+} and ROS in GC cells was markedly increased by HRD1 knockdown (Fig. 5G and 5H). Collectively, these data suggested that HRD1 mediates ACSL4 for ubiquitination and degradation to inhibit ferroptosis.

ATF3 inhibits the transcription of HRD1

As indicated in Fig. 6A, the level of HRD1 in GC tissues was much higher than normal tissues, and HRD1 level in GC tissues was negatively with ATF3 (Fig. 6B). Using JASPAR analysis, we estimated that there was a binding site between HRD1 promoter and ATF3 (Fig. 6C). Luciferase reporter assay revealed that ATF3 significantly decreased the luciferase activity of HRD1 promoter reporter vector group (Fig. 6D). Furthermore, HRD1 promoter was enriched by ani-ATF3 (Fig. 6E). Meanwhile, HRD1 level in GC cells was negatively regulated by ATF3 (Fig. 6F and 6G). Taken together, ATF3 inhibited the transcription of HRD1.

Inhibition of miR-221–3p inhibits the tumor growth of GC in mice

Next, we investigated the role of miR-221–3p in GC progression *in vivo*. In Fig. 7A and 7B, miR-221–3p inhibition markedly attenuated the

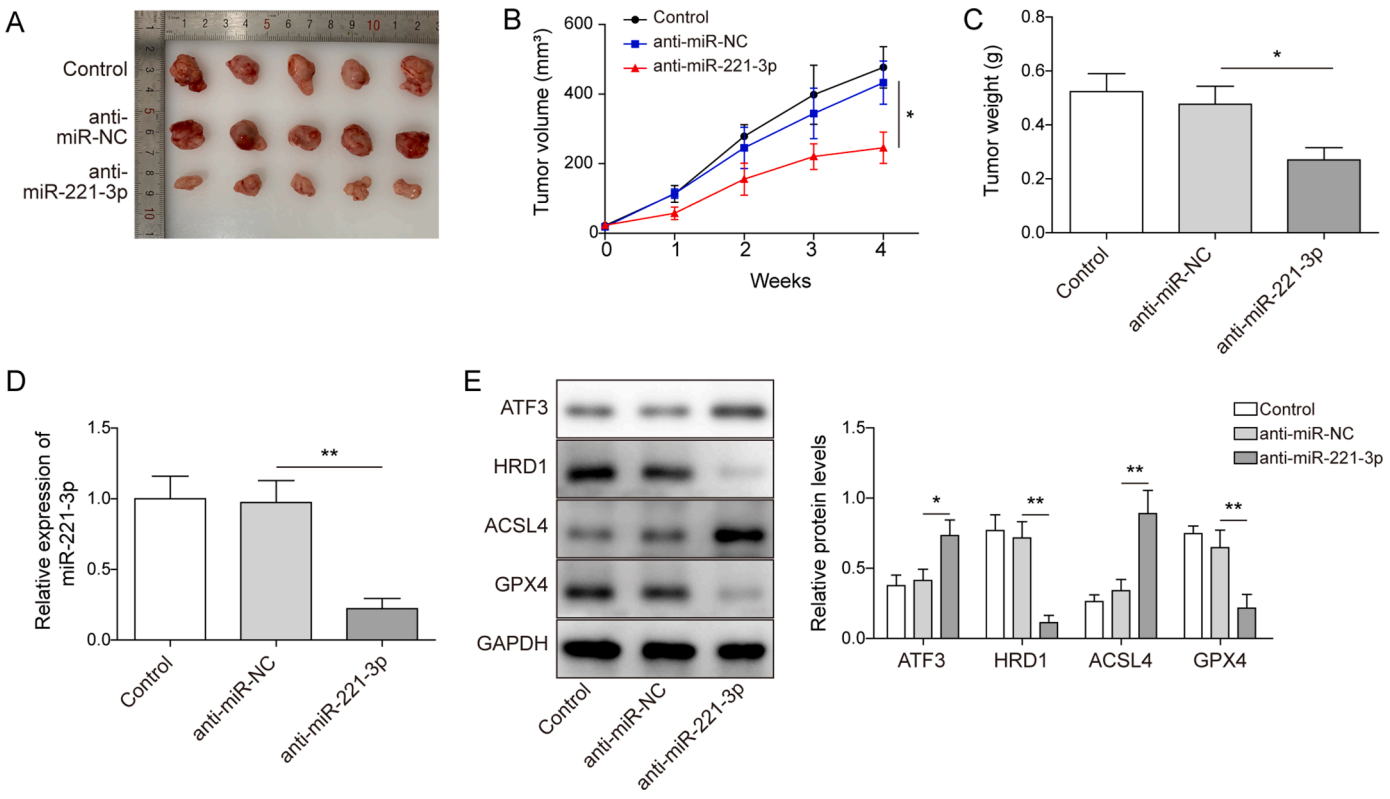

Fig. 7. Inhibition of miR-221–3p inhibits the growth of GC *in vivo*. (A) The tumors of mice were collected and pictured. (B) The volume of tumor in mice was assessed every four days. (C) The weight of tumor was tested. (D) The expression of miR-221–3p in tumor tissues were assessed by RT-qPCR. (E) ATF3, HRD1, ACSL4 and GPX4 levels in tumor tissues were assessed by western blot. *$p<0.05$, **$p<0.01$, ***$p<0.001$.

tumor sizes of mice. Similarly, the tumor weight of mice was notably reduced by miR-221–3p inhibition (Fig. 7C). Meanwhile, the levels of miR-221–3p in tumors were markedly reduced by miR-221–3p inhibition (Fig. 7D). MiR-221–3p inhibition elevated ATF3 and ACSL4 levels but reduced HRD1 and GPX4 levels in tissues of mice (Fig. 7E). In summary, miR-221–3p inhibition suppresses the tumor growth of GC *in vivo*.

Discussion

GC ranks fifth among the prevalent malignancies all over the world [36]. Despite great efforts have been done to study the pathogenesis of GC, the prognosis is still not ideal due to the fact that many patients are diagnosed at an advanced stage [37,38]. Reducing pain and prolonging life are the major treatments in that situation [39,40]. Thus, further studying the molecular mechanisms underlying GC progression can help explore the potential therapeutic targets. This work showed that miR-221–3p depletion could attenuate the tumorigenesis of GC through promoting the ferroptosis. Additionally, miR-221–3p could mediate the transcription of HRD1 and GPX4 via targeting ATF3. HRD1 catalyzed ACSL4 for ubiquitination and degradation to inhibit ferroptosis. Thus, our research confirmed the specific function of miR-221–3p in GC, showing that miR-221–3p could act as an oncogene in GC.

It was reported that ferroptosis could lead to the death in GC cells. Wang J et al. showed that CPEB1 could induce the death in GC cells through promoting the ferroptosis [41]; Mao SH et al. revealed that levobupivacaine could induce the ferroptosis to inhibit the cell growth in GC [42]. Consistently, our study showed that activation of ferroptosis could inhibit the growth of GC cells. On the other hand, miRNAs often participate in the tumorigenesis of GC through regulation of ferroptosis. For example, Ni H et al. found miR-375 could decrease the stemness of GC cells through triggering ferroptosis [43]; Zhang H et al. showed that miR-522 could inhibit ferroptosis in GC [44]. miR-221–3p plays an oncogenic role in GC by inhibiting PTEN or LIFR expression [15,16]. In this research, we found miR-221–3p downregulation could elevate the ferroptosis in GC cells. Inhibition of miR-221–3p suppressed the tumor growth of GC *in vivo*. Thus, we firstly assessed the relation between miR-221–3p and ferroptosis, revealing that miR-221–3p could play a vital role in ferroptosis of GC cells. miRNAs typically inhibit the translation and stability of downstream mRNAs [45]. This work firstly found that ATF3 was the direct target of miR-221–3p. Accumulating evidence showed that ATF3 act as transcriptional repressor [46,47]. In addition, ATF3 also participated in the progression of cancer. It was reported that decreased ATF3 promoted GC progression via increased β-catenin and CEMIP [19]; Di Marcantonio D et al. found that ATF3 could drive the cell cycle distribution in acute myeloid leukemia progression [48]. Furthermore, ATF3 contributes to the ferroptosis [24,49,50]. Consistently, our data showed that ATF3 could inhibit the tumorigenesis of GC. Moreover, our finding also demonstrated that ATF3 could promote the ferroptosis in GC cells. Thus, our research was in line with the above backgrounds. It can be concluded that miR-221–3p downregulation could elevate the ferroptosis in GC cells by targeting ATF3.

HRD1 was upregulated in a variety of tumor tissues [26,27]. Consistently, we also found that HRD1 was obviously increased in GC. Knockdown of HRD1 suppressed GC cell viability. It has been demonstrated that HRD1 mediated various proteins ubiquitination for promoting cancer progression [26,27]. In this study, we found that ATF3 inhibited the transcription of HRD1 in GC. In addition, we found that HRD1 interacted with ACSL4, which is known to be the promoter in ferroptosis. Furthermore, knockdown of HRD1 inhibited ubiquitination and degradation of ACSL4. In addition, knockdown of HRD1 significantly increased the level of erastin-induced Fe^{2+} and ROS in GC cells. These results revealed that HRD1 mediated ACSL4 for ubiquitination and degradation to inhibit ferroptosis.

GPX4 was reported to be the inhibitor during the ferroptosis [23,28,51]. GPX4 downregulation could promote ferroptosis in lung cancer

[52]. GPX4 is a crucial negative regulator of GC cells ferroptosis [53]. Consistent to these results, we found that ATF3 inhibited the transcription of GPX4 in GC.

In conclusion, our research provided a new strategy against GC. However, there is some weakness in this work. Much more targets of miR-221–3p in GC cells need to be explored. To sum up, downregulation of miR-221–3p promotes the ferroptosis in GC cells via upregulation of ATF3 to regulate the transcription of HRD1 and GPX4.

Declarations

Funding

This study was supported by Science and Technology Plan of Suzhou City (SKY2021038), and Primary Research & Social Development Plan of Jiangsu Province (BE2018659).

Ethical approval

All the patients ($n = 32$) signed the informed consent before the experiments. The Ethics Committee of The First Affiliated Hospital of Soochow University approved this research. All *in vivo* experiments were done in line with NIH guide, and Ethics Committees of The First Affiliated Hospital of Soochow University approved this study.

Consent for publication

The informed consent was obtained from study participants.

Availability of data and material

All data generated or analyzed during this study are included in this article. The datasets used and/or analyzed during the current study are available from the corresponding author on reasonable request.

CRediT authorship contribution statement

Chang-Jiang Shao: Conceptualization, Writing – original draft, Methodology, Formal analysis. **Hai-Lang Zhou:** Supervision, Validation, Data curation, Resources. **Xu-Zhu Gao:** Visualization, Investigation, Software. **Chun-Fang Xu:** Funding acquisition, Project administration, Writing – review & editing.

Declaration of Competing Interest

The authors declare that they have no known competing financial interests or personal relationships that could have appeared to influence the work reported in this paper.

Acknowledgements

We would like to give our sincere gratitude to the reviewers for their constructive comments.

References

[1] L. Wu, J. Wang, X. He, Y. Zhu, X. Jiang, Y. Chen, et al., Deep learning system compared with expert endoscopists in predicting early gastric cancer and its invasion depth and differentiation status (with videos), Gastrointest. Endosc. (2021).
[2] S. Du, Z. Fang, L. Ye, H. Sun, G. Deng, W. Wu, et al., Pretreatment neutrophil-to-lymphocyte ratio predicts the benefit of gastric cancer patients with systemic therapy, Aging (Albany NY) (2021) 13.
[3] A. Abouzid, A. Setit, A. Fathi, M. Shetiwy, Laparoscopic partial gastrectomy for large gastric GISTs, J. Gastrointest. Cancer (2021).
[4] S. Ogawa, H. Kubo, Y. Murayama, T. Kubota, M. Yubakami, T. Matsumoto, et al., Matrix metalloprotease-14 is a target enzyme for detecting peritoneal metastasis in gastric cancer, Photodiagnosis Photodyn. Ther. (2021), 102420.
[5] Y. Qin, Y. Qiao, D. Wang, C. Tang, G. Yan, Ferritinophagy and ferroptosis in cardiovascular disease: mechanisms and potential applications, Biomed. Pharmacother. 141 (2021), 111872.
[6] Z. Bao, Y. Liu, B. Chen, Z. Miao, Y. Tu, C. Li, et al., Prokineticin-2 prevents neuronal cell deaths in a model of traumatic brain injury, Nat. Commun. 12 (1) (2021) 4220.
[7] X. Zhu, Y. Zhou, Y. Ou, Z. Cheng, D. Han, Z. Chu, et al., Characterization of ferroptosis signature to evaluate the predict prognosis and immunotherapy in glioblastoma, Aging (Albany NY) (2021) 13.
[8] B. Hassannia, P. Vandenabeele, T. Vanden Berghe, Targeting ferroptosis to iron out cancer, Cancer Cell 35 (6) (2019) 830–849.
[9] Z. Guan, J. Chen, X. Li, N. Dong, Tanshinone IIA induces ferroptosis in gastric cancer cells through p53-mediated SLC7A11 down-regulation, Biosci. Rep. 40 (8) (2020).
[10] S. Hao, J. Yu, W. He, Q. Huang, Y. Zhao, B. Liang, et al., Cysteine dioxygenase 1 mediates Erastin-induced ferroptosis in human gastric cancer cells, Neoplasia 19 (12) (2017) 1022–1032.
[11] M.R. Fabian, N. Sonenberg, W. Filipowicz, Regulation of mRNA translation and stability by microRNAs, Annu. Rev. Biochem. 79 (2010) 351–379.
[12] S. Alizadeh-Fanalou, M. Khosravi, F. Alian, S. Rokhsartalb-Azar, A. Nazarizadeh, M. Karimi-Dehkordi, et al., Dual role of microRNA-1297 in the suppression and progression of human malignancies, Biomed. Pharmacother. 141 (2021), 111863.
[13] X.X. Zhu, X.Q. Yin, G.Z. Hei, R. Wei, Q. Guo, L. Zhao, et al., Increased miR-6875-5p inhibits plasmacytoid dendritic cell differentiation via the STAT3/E2-2 pathway in recurrent spontaneous abortion, Mol. Hum. Reprod. (2021).
[14] C.H. Bao, L. Guo, miR-27b-3p inhibits invasion, migration and epithelial-mesenchymal transition in gastric cancer by targeting runx1 and activation of the hippo signaling pathway, Anticancer Agents Med. Chem. (2021).
[15] J. Shi, Y. Zhang, N. Jin, Y. Li, S. Wu, L Xu, MicroRNA-221-3p plays an oncogenic role in gastric carcinoma by inhibiting PTEN expression, Oncol. Res. 25 (4) (2017) 523–536.
[16] L. Zheng, B. Yan, G. Jin, W. Han, H. Wang, Z. Wang, et al., Circ_0003159 upregulates LIFR expression through competitively binding to miR-221-3p/miR-222-3p to block gastric cancer development, J. Mol. Histol. 53 (2) (2022) 173–186.
[17] Y. Zhang, H. Huang, Y. Zhang, N. Liao, Combined detection of serum MiR-221-3p and MiR-122-5p expression in diagnosis and prognosis of gastric cancer, J. Gastric Cancer 19 (3) (2019) 315–328.
[18] H.C. Ku, C.F. Cheng, Master regulator activating transcription factor 3 (ATF3) in metabolic homeostasis and cancer, Front. Endocrinol. (Lausanne) 11 (2020) 556.
[19] G. Xie, P. Dong, H. Chen, L. Xu, Y. Liu, Y. Ma, et al., Decreased expression of ATF3, orchestrated by beta-catenin/TCF3, miR-17-5p and HOXA11-AS, promoted gastric cancer progression via increased beta-catenin and CEMIP, Exp. Mol. Med. 53 (11) (2021) 1706–1722.
[20] X. Wang, M. Wu, X. Zhang, F. Li, Y. Zeng, X. Lin, et al., Hypoxia-responsive nanoreactors based on self-enhanced photodynamic sensitization and triggered ferroptosis for cancer synergistic therapy, J. Nanobiotechnol. 19 (1) (2021) 204.
[21] Z. Liang, W. Zhao, X. Li, L. Wang, L. Meng, R. Yu, Cisplatin synergizes with PRLX93936 to induce ferroptosis in non-small cell lung cancer cells, Biochem. Biophys. Res. Commun. 569 (2021) 79–85.
[22] W. Li, X. Liu, X. Cheng, W. Zhang, C. Gong, C. Gao, et al., Effect of Malt-PEG-Abz@RSL3 micelles on HepG2 cells based on NADPH depletion and GPX4 inhibition in ferroptosis, J. Drug Target (2021) 1–25.
[23] S. Shui, Z. Zhao, H. Wang, M. Conrad, G. Liu, Non-enzymatic lipid peroxidation initiated by photodynamic therapy drives a distinct ferroptosis-like cell death pathway, Redox. Biol. 45 (2021), 102056.
[24] Y. Wang, F. Quan, Q. Cao, Y. Lin, C. Yue, R. Bi, et al., Quercetin alleviates acute kidney injury by inhibiting ferroptosis, J. Adv. Res. 28 (2021) 231–243.
[25] R.G. Gardner, G.M. Swarbrick, N.W. Bays, S.R. Cronin, S. Wilhovsky, L. Seelig, et al., Endoplasmic reticulum degradation requires lumen to cytosol signaling. Transmembrane control of Hrd1p by Hrd3p, J. Cell Biol. 151 (1) (2000) 69–82.
[26] L. Liu, H. Long, Y. Wu, H. Li, L. Dong, J.L. Zhong, et al., HRD1-mediated PTEN degradation promotes cell proliferation and hepatocellular carcinoma progression, Cell Signal 50 (2018) 90–99.
[27] L. Liu, L. Yu, C. Zeng, H. Long, G. Duan, G. Yin, et al., E3 Ubiquitin Ligase HRD1 Promotes Lung Tumorigenesis by Promoting Sirtuin 2 Ubiquitination and Degradation, Mol. Cell. Biol. 40 (7) (2020).
[28] W. Peng, Z. Zhu, Y. Yang, J. Hou, J. Lu, C. Chen, et al., N2L, a novel lipoic acid-niacin dimer, attenuates ferroptosis and decreases lipid peroxidation in HT22 cells, Brain Res. Bull. 174 (2021) 250–259.
[29] X. Ye, Y. Zhang, X. Wang, Y. Li, Y. Gao, Tumor-suppressive functions of long-chain acyl-CoA synthetase 4 in gastric cancer, IUBMB Life 68 (4) (2016) 320–327.
[30] C. Li, Y. Tian, Y. Liang, Q. Li, Circ_0008035 contributes to cell proliferation and inhibits apoptosis and ferroptosis in gastric cancer via miR-599/EIF4A1 axis, Cancer Cell Int. 20 (2020) 84.
[31] W. Sun, Y. Li, L. Chen, H. Chen, F. You, X. Zhou, et al., ERIS, an endoplasmic reticulum IFN stimulator, activates innate immune signaling through dimerization, Proc. Natl. Acad. Sci. U. S. A. 106 (21) (2009) 8653–8658.
[32] C. Ma, X. Wang, F. Yang, Y. Zang, J. Liu, X. Wang, et al., Circular RNA hsa_circ_0004872 inhibits gastric cancer progression via the miR-224/Smad4/ADAR1 successive regulatory circuit, Mol. Cancer 19 (1) (2020) 157.
[33] S. Lu, Y. Song, R. Luo, S. Li, G. Li, K. Wang, et al., Ferroportin-dependent iron homeostasis protects against oxidative stress-induced nucleus pulposus cell ferroptosis and ameliorates intervertebral disc degeneration in vivo, Oxid. Med. Cell Longev. 2021 (2021), 6670497.
[34] D. Geng, H. Wu, Abrogation of ARF6 in promoting erastin-induced ferroptosis and mitigating capecitabine resistance in gastric cancer cells, J. Gastrointest. Oncol. 13 (3) (2022) 958–967.

[35] X.Z. Yang, T.T. Cheng, Q.J. He, Z.Y. Lei, J. Chi, Z. Tang, et al., LINC01133 as ceRNA inhibits gastric cancer progression by sponging miR-106a-3p to regulate APC expression and the Wnt/beta-catenin pathway, Mol. Cancer 17 (1) (2018) 126.
[36] A. Yang, X. Liu, P. Liu, Y. Feng, H. Liu, S. Gao, et al., LncRNA UCA1 promotes development of gastric cancer via the miR-145/MYO6 axis, Cell. Mol. Biol. Lett. 26 (1) (2021) 33.
[37] B. Wang, Y. Deng, J. Jin, Y. Wu, L Shen, Long noncoding RNA LIT3527 knockdown induces apoptosis and autophagy through inhibiting mTOR pathway in gastric cancer cells, J. Cancer 12 (16) (2021) 4901–4911.
[38] Y. Dang, X. Ouyang, W. Ren, L. Wang, Q. Huang, LncRNA AFAP1-AS1 modulates the proliferation and invasion of gastric cancer cells by regulating AFAP1 via miR-205-5p, Cancer Manag. Res. 13 (2021) 5163–5175.
[39] J. Wu, S. Xu, W. Li, Y. Lu, Y. Zhou, M. Xie, et al., lncRNAs as hallmarks for individualized treatment of gastric cancer, Anticancer Agents Med. Chem. (2021).
[40] M.C. Ba, Z. Ba, Y.F. Gong, K.P. Lin, Y.B. Wu, Y.N. Tu, Knockdown of lncRNA ZNRD1-AS1 suppresses gastric cancer cell proliferation and metastasis by targeting the miR-9-5p/HSP90AA1 axis, Aging (Albany NY) (2021) 13.
[41] J. Wang, T. Wang, Y. Zhang, J. Liu, J. Song, Y. Han, et al., CPEB1 enhances erastin-induced ferroptosis in gastric cancer cells by suppressing twist1 expression, IUBMB Life (2021).
[42] S.H. Mao, C.H. Zhu, Y. Nie, J. Yu, L. Wang, Levobupivacaine induces ferroptosis by miR-489-3p/SLC7A11 signaling in gastric cancer, Front. Pharmacol. 12 (2021), 681338.
[43] H. Ni, H. Qin, C. Sun, Y. Liu, G. Ruan, Q. Guo, et al., MiR-375 reduces the stemness of gastric cancer cells through triggering ferroptosis, Stem Cell Res. Ther. 12 (1) (2021) 325.
[44] H. Zhang, T. Deng, R. Liu, T. Ning, H. Yang, D. Liu, et al., CAF secreted miR-522 suppresses ferroptosis and promotes acquired chemo-resistance in gastric cancer, Mol. Cancer 19 (1) (2020) 43.
[45] G. Di Leva, M. Garofalo, Croce CM. MicroRNAs in cancer, Annu. Rev. Pathol. 9 (2014) 287–314.
[46] M. Bueno, J. Brands, L. Voltz, K. Fiedler, B. Mays, C. St Croix, et al., ATF3 represses PINK1 gene transcription in lung epithelial cells to control mitochondrial homeostasis, Aging Cell 17 (2) (2018).
[47] C.G. James, A. Woods, T.M. Underhill, F. Beier, The transcription factor ATF3 is upregulated during chondrocyte differentiation and represses cyclin D1 and A gene transcription, BMC Mol. Biol. 7 (2006) 30.
[48] D. Di Marcantonio, E. Martinez, J.S. Kanefsky, J.M. Huhn, R. Gabbasov, A. Gupta, et al., ATF3 coordinates serine and nucleotide metabolism to drive cell cycle progression in acute myeloid leukemia, Mol. Cell 81 (13) (2021) 2752–2764, e6.
[49] D. Fu, C. Wang, L. Yu, R. Yu, Induction of ferroptosis by ATF3 elevation alleviates cisplatin resistance in gastric cancer by restraining Nrf2/Keap1/xCT signaling, Cell. Mol. Biol. Lett. 26 (1) (2021) 26.
[50] S. Lu, X.Z. Wang, C. He, L. Wang, S.P. Liang, C.C. Wang, et al., ATF3 contributes to brucine-triggered glioma cell ferroptosis via promotion of hydrogen peroxide and iron, Acta Pharmacol. Sin. (2021).
[51] C.H. Ho, J.H. Huang, M.S. Sun, I.S. Tzeng, Y.C. Hsu, C.Y. Kuo, Wild bitter melon extract regulates LPS-induced hepatic stellate cell activation, inflammation, endoplasmic reticulum stress, and ferroptosis, Evid. Based Complement. Alternat. Med. 2021 (2021), 6671129.
[52] J. Ni, K. Chen, J. Zhang, X. Zhang, Inhibition of GPX4 or mTOR overcomes resistance to Lapatinib via promoting ferroptosis in NSCLC cells, Biochem. Biophys. Res. Commun. 567 (2021) 154–160.
[53] L. Zhao, Y. Peng, S. He, R. Li, Z. Wang, J. Huang, et al., Apatinib induced ferroptosis by lipid peroxidation in gastric cancer, Gastric Cancer 24 (3) (2021) 642–654.